Available online at www.sciencedirect.com
ScienceDirect
Nuclear Instruments and Methods in Physics Research A 585 (2008) 48–60
NUCLEAR INSTRUMENTS & METHODS IN PHYSICS RESEARCH Section A
www.elsevier.com/locate/nima

Study of phenylxylylethane (PXE) as scintillator for low energy neutrino experiments

H.O. Back[a], M. Balata[b], A. de Bari[c], T. Beau[d], A. de Bellefon[d], G. Bellini[e], J. Benziger[f], S. Bonetti[e], A. Brigatti[e], C. Buck[g], B. Caccianiga[e], L. Cadonati[f,2], F. Calaprice[f], G. Cecchet[c], M. Chen[h], A. Di Credico[b], O. Dadoun[d,10], D. D'Angelo[e,3], A. Derbin[j,11], M. Deutsch[k,15], F. Elisei[l], A. Etenko[m], F. von Feilitzsch[i], R. Fernholz[f], R. Ford[f,4], D. Franco[e], B. Freudiger[g,15], C. Galbiati[f], F. Gatti[n], S. Gazzana[b], M.G. Giammarchi[e], D. Giugni[e], M. Göger-Neff[i,*], A. Goretti[b], C. Grieb[i], E. de Haas[f], C. Hagner[i,5], W. Hampel[g], E. Harding[f,13], F.X. Hartmann[g], T. Hertrich[i], H. Hess[i], G. Heusser[g], A. Ianni[b], A.M. Ianni[f], H. de Kerret[d], J. Kiko[g], T. Kirsten[g], G. Korga[e,12], G. Korschinek[i], Y. Kozlov[m], D. Kryn[d], M. Laubenstein[b], C. Lendvai[i], F. Loeser[f], P. Lombardi[e], S. Malvezzi[e], J. Maneira[e,6], I. Manno[o], D. Manuzio[n], G. Manuzio[n], F. Masetti[l], A. Martemianov[m,15], U. Mazzucato[l], K. McCarty[f], E. Meroni[e], L. Miramonti[e], M.E. Monzani[e], P. Musico[n], L. Niedermeier[i,10], L. Oberauer[i], M. Obolensky[d], F. Ortica[l], M. Pallavicini[n], L. Papp[e,12], S. Parmeggiano[e], L. Perasso[e], A. Pocar[f], R.S. Raghavan[p,14], G. Ranucci[e], W. Rau[g,3], A. Razeto[n], E. Resconi[n,7], A. Sabelnikov[e], C. Salvo[n], R. Scardaoni[e], D. Schimizzi[f], S. Schönert[g,1], K.H. Schuhbeck[i,8], E. Seitz[i], H. Simgen[g], T. Shutt[f], M. Skorokhvatov[m], O. Smirnov[j], A. Sonnenschein[f,9], A. Sotnikov[j], S. Sukhotin[m], V. Tarasenkov[m], R. Tartaglia[b], G. Testera[n], D. Vignaud[d], R.B. Vogelaar[a], V. Vyrodov[m], M. Wojcik[q], O. Zaimidoroga[j], G. Zuzel[q]

[a]*Physics Department, Virginia Polytechnic Institute and State University, Robeson Hall, Blacksburg, VA 24061-0435, USA*
[b]*I.N.F.N Laboratori Nazionali del Gran Sasso, SS 17 bis Km 18+910, I-67010 Assergi(AQ), Italy*
[c]*Dipartimento di Fisica Nucleare e Teorica Università and I.N.F.N., Pavia, Via A. Bassi, 6 I-27100 Pavia, Italy*
[d]*Astroparticule et Cosmologie, 10, rue Alice Domon et Leonie Duquet, F-75205 Paris cedex 13, France*
[e]*Dipartimento di Fisica Università and I.N.F.N., Milano, Via Celoria, 16 I-20133 Milano, Italy*
[f]*Department of Physics, Princeton University, Jadwin Hall, Washington Rd, Princeton, NJ 08544-0708, USA*
[g]*Max-Planck-Institut für Kernphysik, Postfach 103 980, D-69029 Heidelberg, Germany*
[h]*Department of Physics, Queen's University Stirling Hall, Kingston, Ont., Canada K7L 3N6*
[i]*Technische Universität München, Physik Department E15, James Franck Straße, D-85747 Garching, Germany*
[j]*Joint Institute for Nuclear Research, 141980 Dubna, Russian Federation*
[k]*Department of Physics, Massachusetts Institute of Technology, Cambridge, MA 02139, USA*
[l]*Dipartimento di Chimica Università, Perugia, Via Elce di Sotto 8, I-06123 Perugia, Italy*
[m]*RRC Kurchatov Institute, Kurchatov Sq. 1, 123182 Moscow, Russian Federation*
[n]*Dipartimento di Fisica Università and I.N.F.N., Genova, Via Dodecaneso, 33 I-16146 Genova, Italy*
[o]*KFKI-RMKI, Konkoly Thege ut 29-33, H-1121 Budapest, Hungary*

*Corresponding author.
E-mail addresses: marianne.goeger@ph.tum.de (M. Göger-Neff), stefan.schoenert@mpi-hd.mpg.de (S. Schönert).

0168-9002/$ - see front matter
doi:10.1016/j.nima.2007.10.045

[p]Bell Laboratories, Lucent Technologies, Murray Hill, NJ 07974-2070, USA
[q]M. Smoluchowski Institute of Physics, Jagellonian University, PL-30059 Krakow, Poland

Received 17 September 2007; received in revised form 23 October 2007; accepted 26 October 2007
Borexino Collaboration
Available online 12 November 2007

Abstract

We report on the study of a new liquid scintillator target for neutrino interactions in the framework of the research and development program of the Borexino solar neutrino experiment. The scintillator consists of 1,2-dimethyl-4-(1-phenylethyl)-benzene (phenyl-o-xylylethane, PXE) as solvent and 1,4-diphenylbenzene (para-Terphenyl, p-Tp) as primary and 1,4-bis(2-methylstyryl)benzene (bis-MSB) as secondary solute. The density close to that of water and the high flash point makes it an attractive option for large scintillation detectors in general. The study focused on optical properties, radioactive trace impurities and novel purification techniques of the scintillator. Attenuation lengths of the scintillator mixture of 12 m at 430 nm were achieved after purification with an alumina column. A radiocarbon isotopic ratio of $^{14}C/^{12}C = 9.1 \times 10^{-18}$ has been measured in the scintillator. Initial trace impurities, e.g. ^{238}U at 3.2×10^{-14} g/g could be purified to levels below 1×10^{-17} g/g by silica gel solid column purification.

PACS: 14.60.Pq; 23.40.−s; 26.65.+t; 29.40.Mc; 91.35.Lj

Keywords: Phenyl-o-xylylethane; PXE; Organic liquid scintillator; Solar neutrino spectroscopy; Low-background counting; Borexino

1. Introduction

Organic liquid scintillators are used in large quantities for rare event detection in particle astrophysics. The main objective in these experiments is the real time spectroscopy of neutrinos from steady-state sources such as the Sun, nuclear reactors and from beta decays in the crust and mantle of the Earth, as well as from transient sources such as supernovae.

Despite the large target mass of several hundreds of tons, the signal rates of the steady-state sources are typically in the range of a few events per day down to a few events per year at MeV or sub-MeV energies. Thus, background signal rates created by radioactivity and cosmic ray interactions need to be extremely low.

Low backgrounds can be achieved by locating the detectors deep underground to suppress the cosmic ray muon flux, shielding the scintillator target against the ambient radioactivity from the surrounding rocks, and suppressing and removing radioactive impurities present in trace amounts in the detector and ancillary systems as well as in the liquid scintillator itself. This concept of background reduction has been pioneered by the Borexino collaboration in the Counting Test Facility (CTF) [1–3] and is implemented in the Borexino detector [4], and similarly, in the KamLAND experiment [5].

This paper summarizes the study of 1,2-dimethyl-4-(1-phenylethyl)-benzene (phenyl-o-xylylethane, PXE), a new scintillator solvent the key characteristics of which are its high density (0.988 g/cm^3) and high flash point (145 °C). This scintillator solvent has been investigated as a 'back-up solution' for the Borexino experiment. The design of choice is based on 1,2,4-trimethylbenzene (pseudocumene, PC), both as buffer liquid and as neutrino target [4].

Since the density of PXE is close to that of water, even large scintillator targets can be submerged in water—serving as a shield against ambient radiation—while creating only modest buoyancy forces on the scintillator containment vessel. Moreover, a detector with water as shield and PXE as target material provides a substantial higher fiducial target mass because of the improved shielding performance against external radiation compared to a detector with identical dimensions, but with both shield and target of organic liquids with standard densities

[1]Also to be corresponded to.
[2]Now at Massachusetts Institute of Technology, NW17-161, 175 Albany St. Cambridge, MA 02139, USA.
[3]Now at Technische Universität München, James Franck Straße, D-85747 Garching, Germany.
[4]Now at Sudbury Neutrino Observatory, INCO Creighton Mine, P.O. Box 159 Lively, Ont., Canada P3Y 1M3.
[5]Now at Universität Hamburg, Luruper Chaussee 149, D-22761 Hamburg, Germany.
[6]Now at Department of Physics, Queen's University Stirling Hall, Kingston, Ont., Canada K7L 3N6.
[7]Now at Max-Planck-Institut fuer Kernphysik, Heidelberg, Germany.
[8]Now at Max-Planck-Institut fuer Plasmaphysik, Boltzmannstr. 2, D-85748 Garching, Germany.
[9]Now at Center for Cosmological Physics, University of Chicago, 933 E. 56th St., Chicago, IL 60637, USA.
[10]Marie Curie fellowship at LNGS.
[11]On leave of absence from St. Petersburg Nuclear Physics Inst., Gatchina, Russia.
[12]On leave of absence from KFKI-RMKI, Konkoly Thege ut 29-33, H-1121 Budapest, Hungary.
[13]Now at Lockhead Martin Corporation, Sunnyvale, CA, USA.
[14]Now at Physics Department, Virginia Polytechnic Institute and State University, Robeson Hall, Blacksburg, VA 24061-0435, USA.
[15]Deceased.

($\sim$0.9 g/cm^3). Finally, a PXE-water configuration reduces the overall inventory of organic liquid in the detector systems, e.g. to about one-fourth in the case of Borexino. This, depending on national regulations, may have an impact on the legal classification of the detector systems and therefore on the safety and operational aspects of the experiment. A further asset of PXE is its high flash point simplifying safety systems relevant for transportation, handling and storage. According to regulations by the United Nations (UN), PXE is legally non-hazardous for transportation purposes and no special United Nation number code applies [6]. In a paper by Majewski et al. [7] PXE has been described as a relatively safe solvent with very low toxicity compared to standard liquid scintillators. The Double Chooz reactor neutrino experiment [8], aiming at a measurement of the mixing angle θ_{13}, will use as target a scintillator mixture based on PXE.

The study reported here of PXE as a solvent for a low-background scintillator for solar neutrino spectroscopy was carried out within the Borexino project. Research on PXE scintillators started in 1995 with laboratory measurements focusing on optical properties and radio purification techniques with solid columns. After completion of the laboratory scale study, about 5 ton of PXE solvent for testing on prototype scale with the CTF of Borexino were acquired in 1996. Fluors were added on site in hall C of the Laboratori Nazionali del Gran Sasso (LNGS) and the final scintillator was purified with Module-0, a solid column purification and liquid handling system [9]. The CTF was loaded with PXE scintillator in October 1996 and first data were acquired until January 1997. The quality of data was limited because only a small fraction of the photomultipliers in the CTF were operational. The PXE scintillator was unloaded from the CTF after the shut down of the detector in July 1997, and moved back into the storage tanks of Module-0. Further batch purification operations were carried out during the period October until December 1997. Samples for neutron activation analysis (NAA) were taken to monitor the achieved radiopurity after each operation. After reconstruction of the CTF during 1999, the PXE scintillator was reloaded into the CTF and measured from June to September 2000. The main objective during this period was the analysis of radiopurity and optical properties in a large volume detector. Beyond this scope, physics limits on electron instability [10], nucleon instability [11], neutrino magnetic properties [12], and on violations of the Pauli exclusion principle [13] could be derived from measurements with the PXE scintillator.

The paper is structured as follows: Section 2 summarizes the physical and chemical properties of the PXE solvent. Section 3 describes the optical properties of the solvent as well as the mixed scintillator. Section 4 is dedicated to the large scale test of the PXE scintillator with the CTF including the scintillator preparation, purification and analysis of trace impurities, and conclusions are given in Section 5.

2. Physical and chemical properties of PXE

PXE is a clear, colorless liquid with an aromatic odor. It is an industrial product with different applications, as for example: insulating oil in high voltage transformers and capacitors and as oil for pressure sensitive paper. PXE is produced by reacting styrene and xylene using an acidic catalyst. It is then washed with water and distilled to improve the purity. Its final industrial purification step uses a solid column.

PXE has the molecular formula $C_{16}H_{18}$ with a weight of 210.2 g/mol. Its molecular structure is shown in Fig. 1.

Chemical and physical details which are of relevance for detector design, safety and operational aspects are listed in Table 1. The key features are its high density of 0.988 g/cm^3, its low vapor pressure and high flash point of 145 °C. It is therefore classified as a non-hazardous liquid.

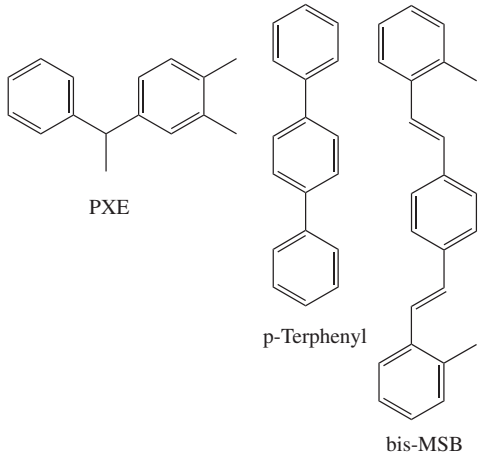

Fig. 1. Molecular structure of 1,2-dimethyl-4-(1-phenylethyl)-benzene (phenyl-o-xylylethane, PXE), 1,4-diphenylbenzene (para-Terphenyl, p-Tp) and 1,4-bis(2-methylstyryl)benzene (bis-MSB).

Table 1
Physical and chemical data of PXE

Cas no.	6196-95-8
Formula	$C_{16}H_{18}$
Molecular weight	210.2 g/mol
Conc. of ortho isomer	99%
Range of density (15 °C)	0.980–1.000 g/cm^3
Typical density (15 °C)	0.988 g/cm^3
Vapor pressure (20 °C)	$<$0.00014 hPa
Vapor pressure (80 °C)	0.13 hPa
Boiling point	295 °C
Flash point	145 °C
Auto-ignition	450 °C
Viscosity (40 °C)	5.2 cSt
Solubility in water (20 °C)	0.01 g/l
Acid no.	$<$0.005 mg KOH/g
Refraction index	1.565

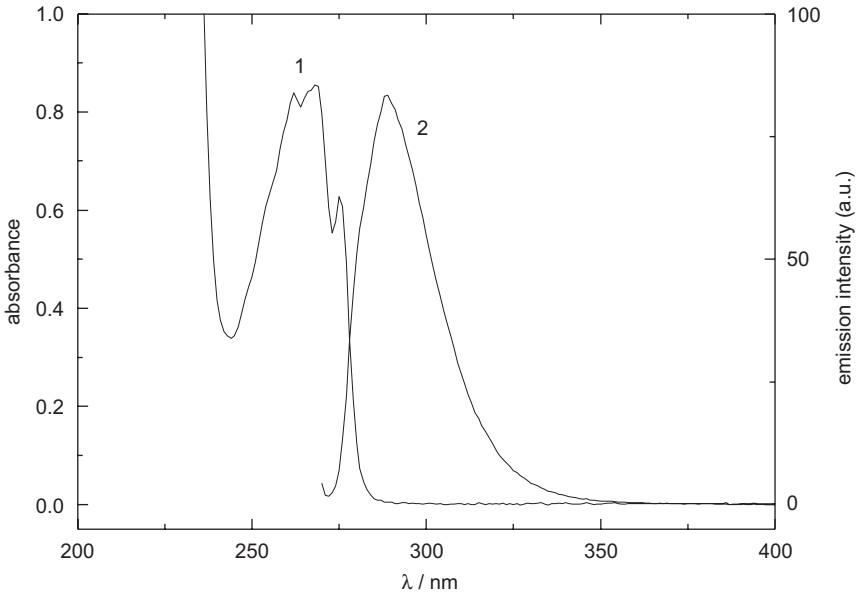

Fig. 2. Absorption (1) and emission (2) spectrum of PXE diluted in cyclohexane.

For our test, the standard production scheme at Koch Chemical Company, Corpus Christi, Texas, USA[16] was modified omitting the final column purification at the company, since it was expected that the clay column material might leach off radioactive impurities, such as uranium and thorium. Instead a column purification system was built and operated using silica gel in the underground laboratories of the LNGS. Details are discussed below.

3. Optical properties

The optical and scintillation properties of the pure PXE solvent, of selected fluors, and of PXE–fluor mixtures have been investigated by UV/Vis spectrometry, by fluorimetry and by excitation with ionizing radiation. The objective was to optimize the scintillator performance by maximizing its light yield and attenuation length and minimizing its scintillation decay time. Methods to remove optical impurities were studied, since impurities can potentially reduce light yield and attenuation length. All optical properties presented in this section are derived from laboratory size samples up to a few hundred milliliters. Attenuation length measurements typically are done in 'one-dimension' only. Scattered light, elastic or inelastic, is undetectable in these measurements, whereas in large volume applications with 4π geometry, the scattered photons are not necessarily lost. The performance of the PXE scintillator in a large volume detector, taking scattering into account, has been studied in CTF and is discussed in Section 4.4.

[16]Koch Special Chemical Company stopped production of PXE in 2002. Dixie Chemical Company Inc., Texas, produces ortho-PXE. Nippon Petrochemicals Co. Ltd., Japan, produces PXE as an equal mixture of ortho, para and meta isomers.

3.1. Solvent properties

PXE diluted in cyclohexane shows an absorption maximum at 267 nm. The emission spectrum after excitation at this wavelength peaks at about 290 nm as displayed in Fig. 2. The fluorescence lifetime after excitation at $\lambda_{exc} = 267$ nm measured in diluted solutions of cyclohexane shows an exponential decay with a lifetime τ of $\sim$22 ns. Preliminary samples obtained from Koch had various optical impurities with absorption bands around 300, 325, 360 and 380 nm. They could be observed both by UV/Vis and fluorimetric measurements. Passing the solvent through a column with acidic alumina reduced the absorption peaks. The band at 380 nm was reduced most efficiently.

The PXE used for the 5 t test, as described in Section 4, still had various optical impurities, but at much reduced levels. The attenuation length at 430 nm (Λ_{430}), defined as $I(x) = I_0 \cdot \exp(-x/\Lambda_{430})$, with the initial intensity I_0 and attenuated intensity $I(x)$ after the optical path length x, was $\Lambda_{430} = 10.2 \pm 0.4$ m in the pure PXE solvent. Attenuation lengths were measured with a Varian Cary 400 UV/Vis photospectrometer in 10 cm cuvettes.

3.2. Scintillator properties

A tertiary scintillator system was chosen in order to shift the emission wavelength to about 430 nm, well above the absorption bands of the residual optical impurities. This is achieved by using 1,4-diphenylbenzene (para-Terphenyl, p-Tp) as primary solute and 1,4-bis(2-methylstyryl)benzene (bis-MSB) as secondary solute. Absorption and emission spectra of PXE in cyclohexane and those of the fluors in PXE are shown in Figs. 2 and 3. The latter shows that the emission spectrum of p-Tp is satisfactorily matched by the absorption spectrum of the wavelength shifter bis-MSB,

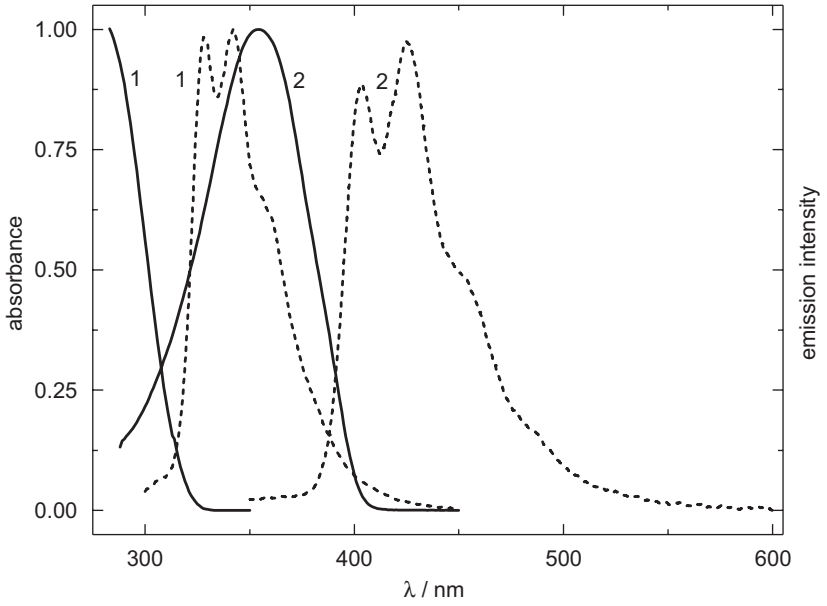

Fig. 3. Absorption (full lines) and emission (dashed lines) spectra of the primary fluor p-Tp (1) and the secondary fluor bis-MSB (2).

Table 2
Parameters of the time profile for photon emission after excitation with alpha and beta particles

Excitation	τ_1	τ_2	τ_3	τ_4	q_1	q_2	q_3	q_4
Beta[a]	3.8	15.9	63.7	243.0	0.832	0.114	0.041	0.013
Beta[b]	3.1	12.4	57.1	185.0	0.788	0.117	0.070	0.025
Alpha[b]	3.1	13.4	56.2	231.6	0.588	0.180	0.157	0.075

[a]PXE/p-Tp (2.0 g/l)/bis-MSB (20 mg/l).
[b]PXE/p-Tp (3.0 g/l)/bis-MSB (20 mg/l).

and therefore an efficient energy transfer is expected in this solvent.

The scintillator properties were tested with p-Tp concentrations at 2 and 3 g/l (close to the solubility limit) and with bis-MSB at 20 mg/l. A scintillation yield of 88 (93)% for PXE with an addition of p-Tp (2.0 (3.0) g/l)/bis-MSB (20 mg/l) with respect to a scintillator based on 1,2,4-trimethylbenzene (PC) and 1.5 g/l of 2,5-diphenyloxazole (PPO) has been found (uncorrected for the PMT sensitivity). Attenuation lengths of $\Lambda_{430} = 2.6$–3.2 m of the scintillator mixture have been measured depending on the sample treatment (cf. Section 4.2).

The fluorescence decay time of the p-Tp (2.0 g/l)/bis-MSB (20 mg/l) scintillator mixture measured by fluorimetry after excitation at 267 nm shows a fast component τ of 3.7 ns. At 3 g/l p-Tp, the decay constant is shortened to 3.2 ns. The photon emission probability density function (pdf) was further studied with ionizing radiation in order to investigate the contribution of long-lived triplet states and the possibility to use the emission time for discrimination of alpha versus beta particles (pulse shape discrimination). The response to gamma radiation has been measured for a concentration of 2.0 and 3.0 g/l p-Tp with a ^{137}Cs source, and to alpha radiation at a concentration of 3.0 g/l using a ^{210}Po alpha source [14,15]. The pdf can be parametrized by the weighted sum of four exponentials $\sum_i (q_i/\tau_i)\exp(-t/\tau_i)$ with the parameters given in Table 2. The emission time distribution is shown in Fig. 4. In addition to an increased slow component which can be used for pulse shape discrimination, alpha particles emit less light because of the high ionization density compared to electron or gamma radiation. The quenching factor is mainly solvent dependent and has been measured for different alpha decays in the ^{238}U chain, using ^{222}Rn loaded scintillator. The results are given in Table 3 [16].

Light attenuation of the standard mixture (PXE/(2.0 g/l)p-Tp/(20 mg/l)bis-MSB) which has been used in the CTF (cf. Section 4) has been measured at various steps during the preparation of the scintillator in 1996 and after filling the CTF. After several purification steps of the mixed scintillator through a silica gel column in Module-0 in order to remove radio-impurities (cf. sections below), attenuation lengths in the range between 2.6 and 3.0 m at 430 nm were measured. After completion of the PXE measurements with CTF and subsequent batch purification operations, the scintillator has been stored in barrels under nitrogen atmosphere. In 2003, this scintillator was used in the frame of the LENS project [17] and optical properties were remeasured to check for degradation with time. The attenuation length as well as the light yield were unchanged with respect to the measurements in 1996. Passing this scintillator mixture through a weak acidic alumina column increased the attenuation lengths to 12 m as displayed in Fig. 5 while retaining the scintillation yield [18].

4. Large scale test of PXE with the Borexino CTF

The main objectives of the large scale test in the Borexino prototype detector (CTF [1]) were the study of

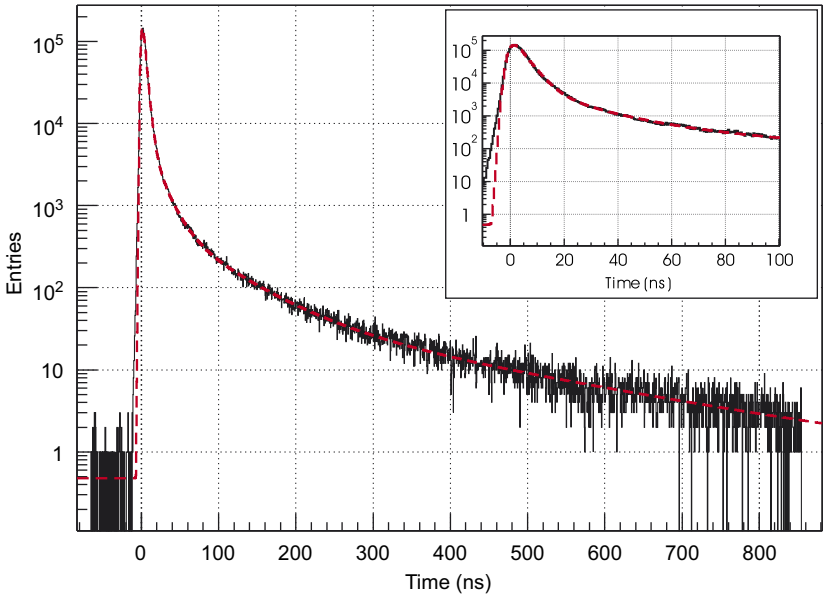

Fig. 4. Photon emission time distribution of PXE/(2.0 g/l)p-Tp/(20 mg/l)bis-MSB scintillator after excitation with gamma radiation from ^{137}Cs decay. The dashed curve shows the fit to the data with a four-exponential decay model. The insert shows enlarged the first 100 ns.

Table 3
Quenching factors for alpha particles with different energies for PXE/p-Tp (2 g/l)/bis-MSB (20 mg/l)

Element	α-Energy (MeV)	Measured energy (keV)	Quenching factor
^{210}Po	5.30	(490 ± 10)	(10.8 ± 0.2)
^{222}Rn	5.49	(534 ± 10)	(10.3 ± 0.2)
^{218}Po	6.00	(624 ± 10)	(9.6 ± 0.2)
^{214}Po	7.69	(950 ± 12)	(8.1 ± 0.1)

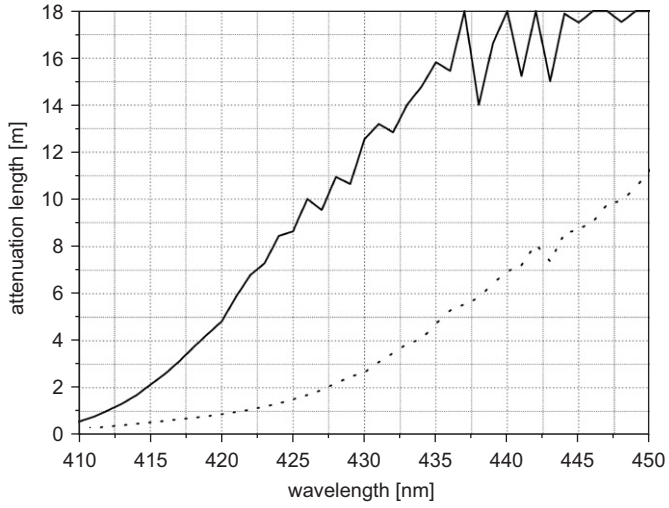

Fig. 5. Attenuation length of the PXE/p-Tp/bis-MSB scintillator before (dashed line) and after (solid line) purification with an alumina column.

(1) optical properties on a large scale, (2) achievable levels of radioactive trace contaminations of the PXE based scintillator, (3) the performance of scintillator purification with a silica gel column, and (4) of the liquid handling system, Module-0. The purity levels required for detection of low-energy solar neutrinos, in particular neutrinos from the ^{7}Be electron capture, are at the μBq/m^3 level corresponding to concentration of ^{238}U and ^{232}Th of $\sim 10^{-16}$ g/g. For detailed specifications of solar neutrino rates and background requirements, the reader is referred to Refs. [4,19]. As the ^{238}U-progenies ^{222}Rn, ^{210}Pb, ^{210}Bi and ^{210}Po are not necessarily in equilibrium with the progenitor activity, we studied the contamination levels of ^{238}U (as well as ^{232}Th and several other isotopes) *directly* with NAA at levels of 10^{-16} g/g and below. The short-lived progenies are not accessible with NAA. Their contamination levels were studied in the CTF together with other backgrounds, as for example the radiogenic produced ^{14}C. New techniques to remove radioactive isotopes by solid column purification were tested for the first time in a ton scale experiment. Furthermore, the preparation, handling and purification of several tons of liquid scintillator with Module-0 was the first test of a subsystem of the liquid handling system to be used in the scintillator operations in Borexino.

4.1. Scintillator preparation

About 5 tons of PXE solvent was procured from Koch Special Chemical Company, Texas, USA. To ensure a controlled procedure, the solvent was loaded by us at the company site in three specially modified and cleaned stainless steel transport containers and shipped to the Gran Sasso underground laboratories.

The PXE solvent was transferred from the transport containers into Module-0, a liquid handling and purification system, specially built for the PXE test. It can be used

for volumetric loading and unloading of liquid scintillator to/from the CTF Inner Vessel (IV), for fluor mixing, purification of liquid scintillator with a silica gel column, Rn degassing of liquid scintillator by nitrogen sparging, and spray degassing as well as for water extraction.

Module-0 consists of a high and low pressure manifold system which are connected by pumps to build up the pressure difference of typically 2 atm. The manifolds are connected to tanks, columns, filters, etc. to allow a variety of flow paths and operations. The system includes two 7 m^3 electropolished pressure tanks (EP1/2), two 1 m^3 process tanks (BT1/2) equipped with nitrogen spargers at the bottom and spray nozzles at the top (for a turbulent injection of liquid together with nitrogen gas), pumps, flow meters, Millipore filters (0.5, 0.1 and 0.05 μm) and one 70 l high pressure column purification unit. All tanks are connected to a high purity nitrogen gas system to provide a nitrogen blanket at typically 30 mbar overpressure. The complete system has been designed according to ultra-high-vacuum standards to avoid contaminations from the environmental air, in particular of ^{222}Rn and ^{85}Kr. Only stainless steel and Teflon are in contact with the liquids. Metal surfaces are electro polished and welds carried out with thorium free welding rods. Module-0 has been constructed in a class 1000 clean room. After completion, all surfaces exposed to scintillator were cleaned following a detailed procedure to remove surface contaminations as radon progenies ^{210}Pb, ^{210}Bi and ^{210}Po. Details about the up-graded system are given in Ref. [9].

The fluors (p-Tp and bis-MSB, both from Sigma-Aldrich Co., scintillation grade) were sieved and then added without further purification to EP1 through a glove box connected to the top inlet flange which was flushed with nitrogen while the PXE solvent was agitated with a nitrogen flux from the bottom inlet to facilitate dissolving p-Tp. To accelerate the solvation of p-Tp, the EP1 tank was heated to 38 °C for four days under continuous nitrogen agitation. The final scintillator mixture had a concentration of 2.0 g/l p-Tp and 20 mg/l bis-MSB.

4.2. Purification with silica gel

One objective of the CTF test was to study the performance of scintillator purification with a solid silica gel column. Preceding laboratory tests of the column purification with PXE/p-Tp with and without the addition of radio tracer showed a clear reduction of metal impurities [20]. The silica gel used during the CTF test has been radio assayed with HP germanium spectrometry and by direct measurements of the emanated radon with proportional counters. The results are listed in Table 4. Despite the high bulk impurities of the Merck silica gel, we did not observe any measurable carry over into the scintillator apart from ^{222}Rn. For further use in Borexino we have found silica gel material with improved radiopurity, in particular a radon emanation rate of 0.13 ± 0.07 mBq/kg.

Table 4
Trace contaminations determined by HP-Ge spectrometry and radon emanation (*) of silica gel 60 from Merck

^{226}Ra	2.28 ± 0.11 Bq/kg
^{222}Rn*	200 ± 10 mBq/kg
^{238}U	1.6 ± 0.3 Bq/kg
^{210}Pb	1.6 ± 0.3 Bq/kg
^{228}Th	1.4 ± 0.1 Bq/kg
^{228}Ra	1.4 ± 0.1 Bq/kg
^{40}K	1.9 ± 0.4 Bq/kg
^{137}Cs	<0.040 Bq/kg

The scintillator components had been mixed as received from the supplier; no special pretreatment had been given to the fluor and the wavelength shifter. The ready mixed PXE scintillator was then passed through a column filled with silica gel (Merck, Silica Gel 60, 25-70 mesh ASTM) at a flow rate of typically 100 l/h. Radon was removed by purging the scintillator after passing the column as displayed schematically in Fig. 6. Samples for NAA were taken prior and after all major steps of the scintillator preparation and purification: *Sample* (1) was collected from Module-0 after addition of p-Tp and bis-MSB to the PXE solvent (without purification). *Sample* (2) was collected during the filling of the IV. The total amount of scintillator had passed once a column of about 80 cm height (15 kg) which had been exchanged against fresh silica gel after the first 2 ton had run through the column, and once with a height of about 50 cm, i.e. in total two times. *Sample* (3) has been taken after the scintillator was circulated from the IV through the column (re-filled to a height of 80 cm) and back into the IV. The flow rate was adjusted such that one cycle (5000 l) took two days. The scintillator was circulated for four days, i.e. two cycles. Subsequently the scintillator was unloaded from the IV into the EP1-tank. *Sample* (4) was taken after completion of a water extraction in the EP1 tank. *Sample* (5) was collected in Module-0 after circulating the scintillator from EP1 through the column back to EP1. The column packing had not been exchanged (same as in (3)). This final operation lasted for eight days with a flow rate of 3600 l/day, i.e. about six cycles.

4.3. Radioassay with NAA

Combining neutron activation and low level counting methods, we developed a novel analytical method with sensitivities of 10^{-16} g/g and below for ^{238}U and ^{232}Th in liquid scintillators. For this purpose about 250 g samples of liquid scintillator were irradiated at a neutron flux of $(10^{12}-10^{13})\,s^{-1}\,cm^{-2}$ up to 100 h at the research reactor in Garching. The long-lived primordial radionuclides are transformed into short-lived radionuclides (e.g. $^{238}U \rightarrow {}^{239}Np$, $^{232}Th \rightarrow {}^{233}Pa$), thus providing a higher specific activity with respect to their progenitors. After irradiation, liquid–liquid and ion exchange techniques were applied to separate the radionuclides of interest

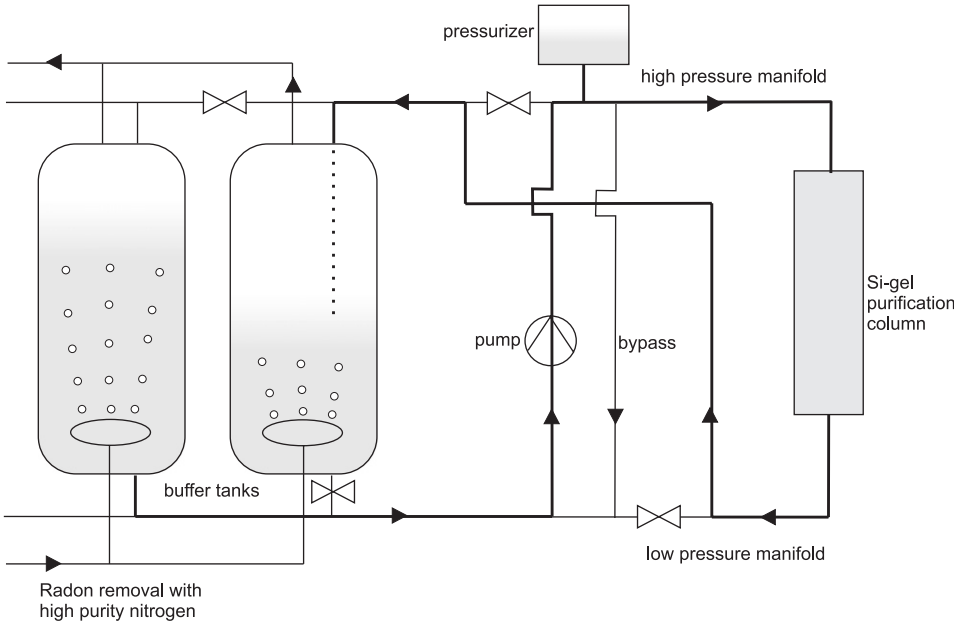

Fig. 6. Flow path of PXE scintillator during column purification with subsequent nitrogen stripping in Module-0.

Table 5
Concentration of trace elements in the PXE scintillator

Element	Concentration (g/g)				
	1	2	3	4	5
Th	$<2\times10^{-14}$	$(5.0\pm2.5)\times10^{-15}$	$<3\times10^{-15}$	$(2.5\pm0.7)\times10^{-16}$	$<1.8\times10^{-16}$
U	$(4.0\pm2.0)\times10^{-14}$	$(1.4\pm0.7)\times10^{-15}$	$<6\times10^{-16}$	$<2.5\times10^{-16}$	$<1\times10^{-17}$
Cd	ND	$<2\times10^{-12}$	ND	$<5.4\times10^{-14}$	$<8.3\times10^{-15}$
In	$<3\times10^{-13}$	$(5.0\pm2.5)\times10^{-12}$	$<4.8\times10^{-13}$	$<2.5\times10^{-14}$	$<1.2\times10^{-13}$
K	$<8\times10^{-12}$	$<5\times10^{-11}$	$<1.3\times10^{-11}$	$<2\times10^{-12}$	$<6.1\times10^{-12}$
La	$<3\times10^{-14}$	$<2\times10^{-14}$	$<6.4\times10^{-15}$	$<9.4\times10^{-16}$	$<4.3\times10^{-16}$
Lu	$<2\times10^{-15}$	$<7\times10^{-16}$	$<1.4\times10^{-15}$	$<4.0\times10^{-16}$	$<3.8\times10^{-16}$
Rb	$<3\times10^{-13}$	$<8\times10^{-12}$	$<2.8\times10^{-13}$	$<1.1\times10^{-13}$	$<1.2\times10^{-13}$
Ag	$<1\times10^{-12}$	$<2\times10^{-12}$	$(7.9\pm3.0)\times10^{-14}$	$(1.1\pm0.5)\times10^{-13}$	$(2.3\pm0.4)\times10^{-13}$
Au	$(2.0\pm1.0)\times10^{-14}$	$(2\pm1)\times10^{-15}$	ND	$(1.8\pm0.9)\times10^{-16}$	$<3.8\times10^{-17}$
Cr	ND	$(3\pm1.5)\times10^{-11}$	$<1\times10^{-13}$	$(1.9\pm0.9)\times10^{-13}$	$(2.3\pm0.4)\times10^{-13}$
Fe	$<2\times10^{-10}$	$<2\times10^{-10}$	ND	$<2.5\times10^{-12}$	$(3.7\pm0.6)\times10^{-11}$
Sb	$(3.0\pm1.5)\times10^{-13}$	$(3.0\pm1.5)\times10^{-13}$	ND	$(3.0\pm1.5)\times10^{-14}$	$(8.7\pm1.3)\times10^{-15}$
W	ND	$(1.0\pm0.5)\times10^{-13}$	ND	$(1.4\pm0.9)\times10^{-14}$	$<4.8\times10^{-15}$
Zn	ND	$(7.0\pm3.5)\times10^{-11}$	ND	$(3.1\pm0.5)\times10^{-13}$	$(1.0\pm0.2)\times10^{-12}$

The samples were taken during the scintillator preparation and purification processes (cf. Section 4.2). The upper part lists elements with long-lived radioactive isotopes which are a potential background in Borexino, the lower part lists some non-radioactive elements for illustration of the cleaning performance. ND: no data, limits: 90% CL, errors: 1σ.

from interfering activities. Coincidence counting methods [21], e.g. β–γ-conversion electron for ^{239}Np and β–γ for ^{233}Pa, further increase the sensitivity. Details can be found in Refs. [19,22,23].

The main results of the NAA of the scintillator samples (1)–(5) are summarized in Table 5 [24]. We report the concentrations of ^{238}U, ^{232}Th and other long-lived isotopes which contribute to the background in Borexino. In order to illustrate the performance of the silica gel column, also the concentrations for several non-radioactive metal isotopes are given. An overall reduction between 1 and 3 orders of magnitude has been reached for all elements where a positive value (above the detection limit) could be measured before the purification. Except for potassium, where the purity needed for Borexino is below the detection limit of the NAA, the requirements for Borexino are met for all of the long-lived radionuclides. New purity records in organic liquid scintillators have been achieved for

uranium at $c(^{238}\mathrm{U}) < 1 \times 10^{-17}$ g/g, and for thorium at $c(^{232}\mathrm{Th}) < 1.8 \times 10^{-16}$ g/g.

4.4. Measurements of PXE scintillator in the CTF

The Borexino prototype detector CTF is a highly sensitive instrument for the study of backgrounds in liquid scintillators at energies between a few tens of keV and a few MeV. It consists of a transparent nylon balloon with 2 m diameter containing 4.2 m^3 of liquid scintillator (IV). One hundred PMTs with light concentrators mounted on a 7 m diameter support structure detect the scintillation signals (optical coverage 20%). The whole system is placed inside a cylindrical steel tank (11 m in diameter, 10 m in height) that contains 1000 ton of ultra-pure water in order to shield against external γ rays from the PMTs and other construction material as well as neutrons from the surrounding rock. In the upgraded version of the CTF detector (after 1999), 16 additional PMTs mounted on the floor of the water tank detect the Cherenkov light created by muons transversing the water buffer and are used as a muon veto. Details of the CTF detector and results of first measurements with pseudocumene scintillator are given in Refs. [1,3].

4.4.1. Sequence of measurements

Direct counting after first loading of the PXE scintillator into the CTF in 1997 did not provide conclusive results because of phototube and electronics problems of the detector system that hindered data evaluation. After an upgrade of the CTF detector and the liquid handling system during 1998 and 1999, the same scintillator was filled again into the CTF in summer 2000, after passing once through a 40 l silica gel column. The loading of the scintillator into the IV was done in four batches of 1 ton each separated by short periods of data taking. Undisturbed data taking with 4.2 ton of PXE were going on from July 16 until September 5, 2000, in total 52 days. Afterwards, a series of calibration measurements with a ^{222}Rn point source were carried out where the source was moved inside the IV to map the detector response and tune the position reconstruction software.

4.4.2. Detector performances

The pulse height–energy relation can be derived from the ^{214}Po alpha peak together with the measured quenching factors as given in Table 3. Due to its short half life of 164 μs, the ^{214}Po decay can easily be tagged. The ^{214}Po stems mainly from ^{222}Rn introduced during scintillator loading and therefore is homogeneously distributed in the scintillator volume. The alpha particle has an energy of 7.69 MeV which in the scintillator is quenched to an equivalent beta energy of (950 ± 12) keV. The measured peak position in the CTF corresponds to (304 ± 3) photoelectrons leading to a yield of (320 ± 8) photoelectrons per MeV. The pulse height–energy relation is also a parameter of the ^{14}C fit (see below), which is done in the energy range from 70 to 150 keV, resulting in a somewhat higher value of 340 photoelectrons per MeV. A more detailed analysis of the photoelectron yield including a model with ionization quenching, has been presented in Ref. [12]. A value of 372 ± 8 photoelectrons per MeV has been derived for the asymptotic yield, i.e. for scintillation light created by electrons with energies large compared to their rest mass.

The energy resolution derived from the width of the ^{214}Po alpha peak corresponds to $\sigma(E)/E \simeq 8.7\%$, or $\sigma(E)/\sqrt{E} \simeq 2.6\,\mathrm{keV}^{1/2}$. It is expected to scale with $\sqrt{(E)}$. A similar value of $\sigma(E)/\sqrt{E} \simeq 2.5\,\mathrm{keV}^{1/2}$ is obtained from the spectral analysis of the ^{14}C spectrum.

The spatial resolution was studied with a localized ^{222}Rn source at various positions inside the IV [25]. Values of $\sigma_{x,y} \simeq 12$ cm, $\sigma_z \simeq 13$ cm at 600 keV were obtained at the detector's center (cf. Fig. 7). The spatial resolution degrades up to 15% close to the surface of the IV.

The photon arrival time distribution was studied with the source located at the center of the detector. Fig. 8 displays the time distribution for scintillation photons from the ^{214}Bi beta decay. The data are compared with a Monte Carlo simulation which includes the scintillation decay time from laboratory measurements given in Table 2, elastic and inelastic scattering and the PMT time jitter. Monte Carlo and data show good agreement for arrival times up to 25 ns. The data show a larger slow component than the MC simulation, which could be due to reflected

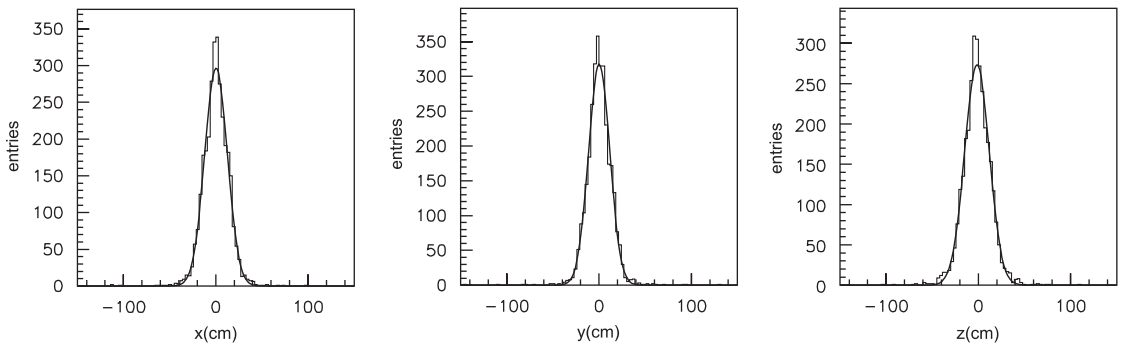

Fig. 7. Reconstructed position (x, y, z) of ^{214}Po events during a run with a ^{222}Rn source at the detector's center.

photons and/or PMT late pulses which are not fully accounted for in the simulation.

To distinguish alpha from beta particles by pulse shape discrimination, the analog sum of the charge signal from all PMTs is split into three identical signals and fed into a charge sensitive ADC with different time delays. The total charge is derived from integration over the entire charge signal 0–500 ns, while the slow component is derived from the time windows 32–532 and 48–548 ns, respectively.

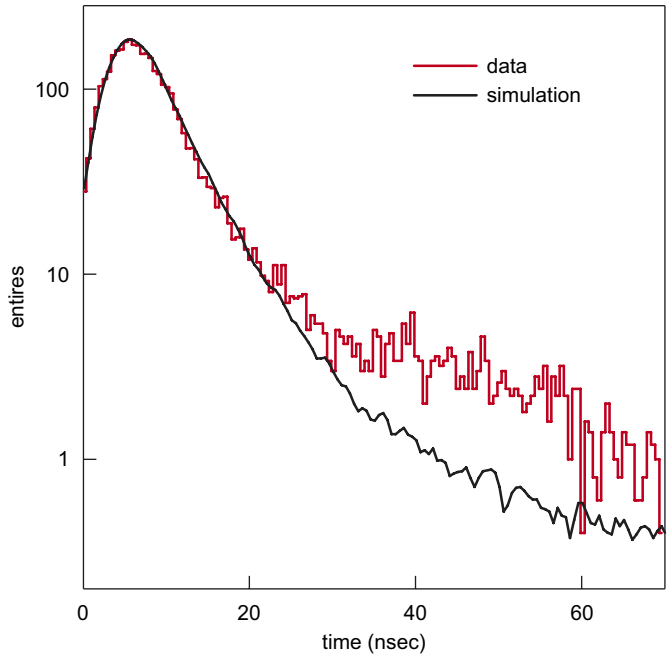

Fig. 8. Arrival time distribution of scintillation photons after excitation with β/γ from ^{214}Bi decay at the detector's center. The red (gray) line corresponds to CTF data and the black curve to MC simulation.

The tail-to-total ratio $r_{32/\mathrm{tot}}$ or $r_{48/\mathrm{tot}}$ can then be used as discrimination parameter [26] as displayed in Fig. 9. The discrimination efficiency can be derived from a clean data sample of α and β/γ events in the corresponding energy range. Only the ^{214}Bi(β)–^{214}Po(α) decay sequence can unambiguously be identified as pure α or β/γ events due to the short half life of ^{214}Po. Only ^{214}Bi events in the same energy range as the ^{214}Po events (0.6–1.3 MeV) were considered. Fixing the β acceptance efficiency at 98% leads to an α identification efficiency of 84.6%; applying a radial cut on the ^{214}Bi and ^{214}Po events of $r<90$ cm leads to an increased α identification efficiency of 92.4%. This improvement is due to the fact that for events in the outer regions of the IV the difference in the light path to different PMTs is higher, and therefore the fraction of light registered at late times is higher. Also other methods for α/β discrimination like the Gatti optimum filter method have been studied with the CTF [27,28], and will be implemented in Borexino.

4.4.3. Radiopurity analysis

The counting rate below 200 keV is dominated by the ^{14}C beta decay with an endpoint of 156 keV. The ^{14}C concentration in the scintillator was determined by fitting a convolution of the theoretical beta spectrum and the energy dependent detector resolution function, plus a background contribution to the measured spectrum in the energy range from 70 to 150 keV [2,29]. The low energy spectrum together with the fit is displayed in Fig. 10. At energies below 70 keV there is a background contribution from Cherenkov events produced by γ's in the shielding water. From the fit we derive the ^{14}C activity which translates to a ratio of $^{14}\mathrm{C}/^{12}\mathrm{C} = (9.1 \pm 0.3(\mathrm{stat}) \pm 0.3(\mathrm{syst})) \times 10^{-18}$. The systematic error is dominated by the uncertainty of the total scintillator mass.

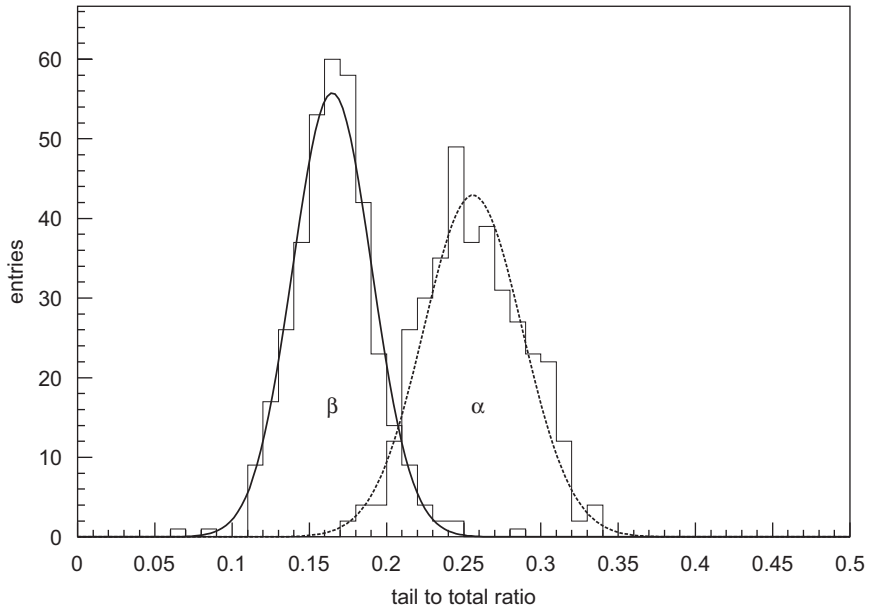

Fig. 9. Tail-to-total-ratio $r_{48/\mathrm{tot}}$ of ^{214}Bi β/γ and ^{214}Po α events. Only β/γ events with energy deposition between 0.6 and 1.3 MeV are included.

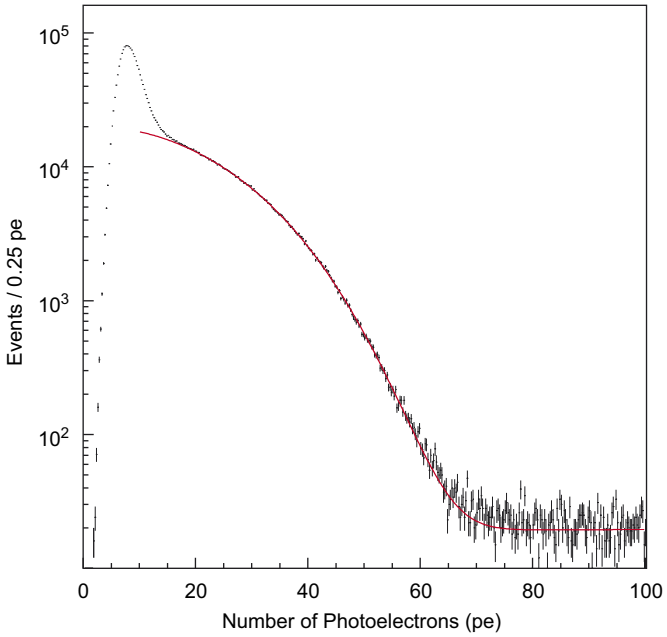

Fig. 10. The low energy spectrum collected during a period of 6.4 days. The counting rate is dominated by the ^{14}C β-decay with $^{14}C/^{12}C = (9.1 \pm 0.3(\text{syst}) \pm 0.3(\text{stat})) \times 10^{-18}$. The solid line shows the fit of the theoretical ^{14}C spectrum to the data.

The ^{238}U decay chain is assayed via the delayed coincidence of the ^{222}Rn progenies ^{214}Bi(β/γ) and ^{214}Po(α) with a half life of 164 μs. Assuming secular equilibrium of the decay chain—which is likely to be broken due to the long-lived ^{226}Ra and the gaseous ^{222}Rn—the measured ^{214}Bi–^{214}Po activity can be expressed as uranium-equivalent. After loading the CTF an initial ^{214}Bi–^{214}Po rate of about 90 counts per day was observed which was clearly related to ^{222}Rn introduced during the filling process, as it decayed away with the ^{222}Rn half life of 3.8 days. The last two 1-week-periods of data taking with a total counting time of 7.32 days (period I) and 6.98 days (period II) were used for the analysis, when the contribution from the initial ^{222}Rn contamination was below 1 count per day. The detector efficiency (due to the dead time connected with the read out of each event) was 91% during that period. The ^{214}Bi–^{214}Po events were selected by applying the following cuts: no muon veto trigger (efficiency > 99%); energy of the first event > 300 keV (efficiency 95%); energy of the following event between 0.6 and 1.25 MeV (99%); coincidence time between 5 and 800 μs (94%). Two hundred and twenty four (199) candidate events survived the cuts for period I (II), corresponding to a ^{222}Rn activity of 102 μBq/m^3 (99 μBq/m^3). This activity, however, was not homogeneously distributed within the scintillator volume, but most of the events were localized along the vertical symmetry axis of the detector. An artifact due to false reconstruction could be excluded after calibration with point-like sources which were located both on and off axis. Though the origin of these events could not be fully resolved, it is excluded that they are related to the intrinsic scintillator impurities. To derive a number for the residual ^{222}Rn concentration homogeneously distributed in the scintillator, a cylindrical cut around the vertical axis was applied. For $R_{x,y} > 0.6$ m we get a ^{222}Rn activity of $A(^{222}\text{Rn}) = (27 \pm 5)$ μBq/m^3 in period I and $A(^{222}\text{Rn}) = (23 \pm 5)$ μBq/m^3 in period II, or a ^{238}U equivalent concentration of $c(^{238}\text{U}) = (2.3 \pm 0.4) \times 10^{-15}$ g/g (I) and $c(^{238}\text{U}) = (1.9 \pm 0.4) \times 10^{-15}$ g/g (II). Due to the above stated ^{222}Rn problem this value must be considered as an upper limit of the internal ^{238}U contamination.

Further radio-isotopes from the uranium decay chain of concern are the ^{210}Pb progenies ^{210}Bi and ^{210}Po. Secular equilibrium typically is disturbed even within this sub-chain, as well as with respect to the progenitor ^{226}Ra because of the characteristic lifetimes and the different chemistries involved. From a spectral analysis, about 100–200 decays per day with alpha-like pulse shapes and with energy depositions quenched to approximately 0.5 MeV are attributed to ^{210}Po decays in the scintillator [30].

A limit for the intrinsic ^{232}Th contamination can be derived via the delayed β–α coincidence of its progenies ^{212}Bi–^{212}Po with a half life of 299 ns. It can be distinguished from the ^{214}Bi–^{214}Po coincidence by the higher energy of the α decay and the shorter coincidence time, though the latter has to be considered as a background. Secular equilibrium in the ^{232}Th chain is usually observed for ^{228}Th and its progenies. The following cuts were applied to select the ^{212}Bi–^{212}Po events: no muon veto trigger; energy of the first event > 300 keV (efficiency 85%); energy of the second event > 800 keV (100%); coincidence time between 50 and 1500 ns (86%); due to a contamination at the bottom of the vessel only decays in the upper hemisphere of the detector were considered (50%). The overall efficiency of the cuts for the selection of the ^{212}Bi–^{212}Po events is 37%. During the whole period of undisturbed data taking, in total 25.8 days of live time, 12 candidates were detected, leading to a ^{232}Th equivalent concentration of $c(^{232}\text{Th}) = (1.3 \pm 0.4) \times 10^{-15}$ g/g.

An estimation of the remaining background for the neutrino detection in Borexino is provided by the subtraction of all known contributions from the background spectrum measured in the CTF. In order to reduce the contribution from the external background, a radial cut ($r < 0.9$ m) has been applied. Also, all correlated events have been tagged and discriminated. In the neutrino window (NW, 250 keV < E < 800 keV), the counting rate then is 120 events per day and ton. As next step, all muon induced events have been subtracted (74 events per day and ton). In this inner region of the detector, alphas can be discriminated via their pulse shape with an efficiency of ~90%, leading to 48 events per day and ton. The resulting background spectrum is shown in Fig. 11. Clearly visible are the contributions from ^{14}C the remaining alphas from the ^{238}U and ^{232}Th chain, and a ^{40}K γ peak, which could be identified as external background originating from the Vectran strings that hold the IV in place (a dedicated measurement of the strings showed a concentration of 45 ppm K).

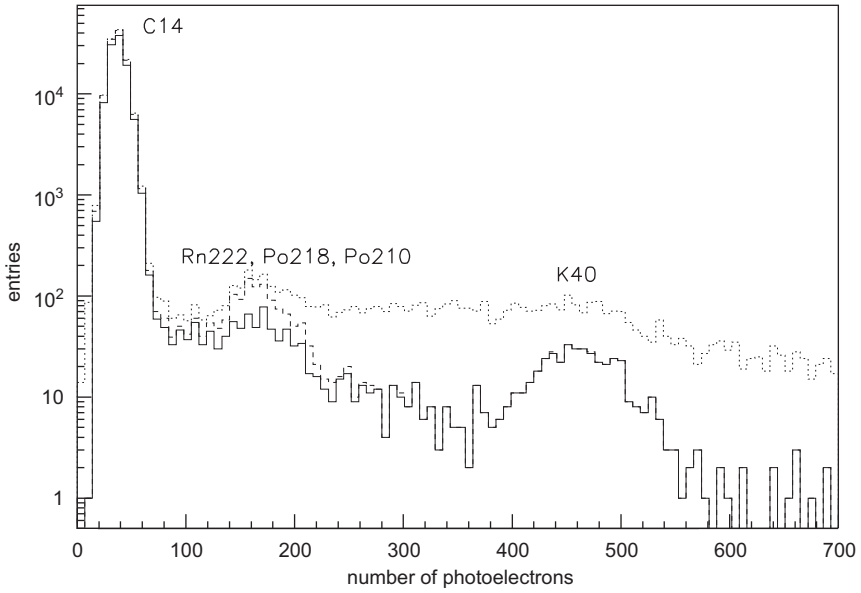

Fig. 11. PXE data collected in a period of 7.3 days. Only single events with $r<90$ cm are shown (dotted line). In the next step, all muon events are removed (dashed line). In the final step 90% of the alpha events are subtracted via pulse shape analysis (solid line).

4.4.4. Summary of CTF results

The large scale test of a scintillator based on PXE in the CTF showed that its optical properties (light yield of ~340 pe/MeV at 20% coverage, position resolution ~12 cm at 600 keV, α/β-separation >90%) make it a good target scintillator for the spectroscopy of low energetic neutrinos. The purity levels required for the detection of low energy solar neutrinos can be achieved by purification of the scintillator with a silica gel column. Though the very low ^{238}U and ^{232}Th concentrations measured by NAA ($<1\times10^{-17}$ g/g and $<2\times10^{-16}$ g/g) could not be confirmed by the CTF measurements, the remaining activity levels were close to the detector's sensitivity limit and largely influenced by systematics e.g. due to external background and surface contamination.

5. Outlook

PXE based scintillator has been investigated for application in Borexino as detector medium for low energy solar neutrino spectroscopy. Key questions under study were the optical properties, radiopurity and new techniques of purification by solid column extraction. Both laboratory measurements and the large scale operations in the CTF showed that PXE scintillator as target and water as buffer medium is a viable solution for Borexino and it was rated as a backup solution.[17]

Because of its superior safety characteristics and the better self-shielding due to its higher density, future applications of PXE in underground experiments are conceivable, as for example the search for non-vanishing value of θ_{13} with reactor neutrinos, the search for neutrinoless double beta decay with metal loaded scintillators, the study of neutrinos from the interior of the Earth and from Supernovae, as well as the study of proton decay via the K-meson decay channel.

[17]The default configuration in the Borexino design is based on pseudocumene as scintillator as well as buffer medium.

Acknowledgments

F.X. Hartmann would like to thank the extra-ordinary services of the Koch Speciality Chemical Company and the ALCOA Company as regards the solid column design.

References

[1] G. Alimonti, Borexino Collaboration, et al., Nucl. Instr. and Meth. A 406 (1998) 411.
[2] G. Alimonti, Borexino Collaboration, et al., Phys. Lett. B 422 (1998) 349.
[3] G. Alimonti, Borexino Collaboration, et al., Astropart. Phys. 8 (1998) 141.
[4] G. Alimonti, Borexino Collaboration, et al., Astropart. Phys. 16 (2002) 205.
[5] K. Eguchi, KamLAND Collaboration, et al., Phys. Rev. Lett. 90 (2003) 021802.
[6] See for example: United States Code of Federal Regulations, Title 49, vol. 2, part 173.
[7] S. Majewski, et al., Nucl. Instr. and Meth. A 414 (1998) 289.
[8] F. Ardellier, et al., Double Chooz collaboration, hep-ex0606025.
[9] F.X. Hartmann, in: W. Hampel (Ed.), Proceedings of the Fourth International Neutrino Conference, MPIK Heidelberg, Heidelberg, 1997, p. 202;
L. Niedermeier, et al., Nucl. Instr. and Meth. A 568 (2006) 915.
[10] H.O. Back, Borexino Collaboration, et al., Phys. Lett. B 525 (2002) 29.
[11] H.O. Back, Borexino Collaboration, et al., Phys. Lett. B 563 (2003) 23.
[12] H.O. Back, Borexino Collaboration, et al., Phys. Lett. B 563 (2003) 35.
[13] H.O. Back, Borexino Collaboration, et al., Eur. Phys. J. C 37 (2004) 421.

[14] P. Lombardi, Diploma Thesis, Universita di Milano, 1996.
[15] D. Motta, Ph.D. Thesis, MPIK Heidelberg, 2004.
[16] M. Neff, Diploma Thesis, Technische Universität München, 1996.
[17] C. Buck, F.X. Hartmann, D. Motta, S. Schönert, U. Schwan, Nucl. Phys. B (Proc. Suppl.) 118 (2003) 451.
[18] C. Buck, Ph.D. Thesis, MPIK Heidelberg, 2004.
[19] C. Arpesella, Borexino Collaboration, et al., Astropart. Phys. 18 (2003) 1.
[20] T. Goldbrunner, Ph.D. Thesis, Technische Universität München, 1997.
[21] R.S. Raghavan, et al., AT & T Bell Laboratories, Technical Memorandum, 11121-921015-37, 1992.
[22] T. Goldbrunner, et al., Nucl. Phys. B (Proc. Suppl.) 61 (1998) 176.
[23] R.v. Hentig, et al., Nucl. Phys. B (Proc. Suppl.) 78 (1999) 115.
[24] R.v. Hentig, Ph.D. Thesis, Technische Universität München, 1999.
[25] M. Göger-Neff, Ph.D. Thesis, Technische Universität München, 2001.
[26] G. Ranucci, et al., Nucl. Instr. and Meth. A 412 (1998) 374.
[27] M. Monzani, Diploma Thesis, Universita di Milano, 2001.
[28] T. Beau, Ph.D. Thesis, Université Paris 7, 2002.
[29] E. Resconi, Ph.D. Thesis, Universita di Genova, 2001.
[30] L. Cadonati, Ph.D. Thesis, Princeton University, 2000.